emission process, such as the comptonization model discussed, would favour the identification of Cyg X-1 with a black hole or other object without a strong magnetic field, which would modify the spectrum through cyclotron processes. The spectrum of a thermal process would be cut off at an energy determined by the maximum temperature. Our observations show that such a maximum temperature must be at least in the neighbourhood of 50–100 keV, approximately the largest value allowed by current theory[12].

This work was supported by NASA contract NAS 8-27974.

Received 17 June; accepted 5 August 1981.

1. Oda, M. *Space Sci. Rev.* **20**, 757–813 (1977).
2. Dolan, J. F., Crannell, C. J., Dennis, B. R., Frost, K. J. & Orwig, L. E. *Astrophys. J.* **230**, 551–557 (1979).
3. Shapiro, S. L., Lightman, A. P. & Eardley, D. M. *Astrophys. J.* **204**, 187–199 (1976).
4. Sunyaev, R. A. & Titarchuk, L. G. *Astr. Astrophys.* **86**, 121–138 (1980).
5. Sunyaev, R. A. & Trümper, J. *Nature* **279**, 506–508 (1979).
6. Rothschild, R. *et al. Space Scient. Instrum.* **4**, 269–301 (1979).
7. Matteson, J. L. *Proc. AIAA 16th Aerospace Sciences Meeting*, Huntsville, Paper 78–35 (1978).
8. Meegan, C. A., Fishman, G. J. & Haymes, R. C. *Astrophys. J. Lett.* **234**, L123–128 (1978).
9. Haymes, R. C. & Harnden, F. R. *Astrophys. J.* **159**, 1111–1114 (1970).
10. Mandrou, P., Neil, M., Vedrenne, G., Dupont, A. & Hurley, K. *Astrophys. J.* **219**, 288–291 (1978).
11. Baker, R. E., Lovett, R. R., Orford, K. J. & Ramsden, D. *Nature phys. Sci.* **245**, 18–19 (1973).
12. Liang, E. P. T. *Astrophys. J.* **234**, 1105–1112 (1979).

Can the twin-exhaust model explain radio jets?

Michael D. Smith*, Larry Smarr†, Michael L. Norman‡ & James R. Wilson§

*† Department of Physics and † Department of Astronomy, University of Illinois, Urbana, Illinois 61801, USA
‡ Department of Applied Science, University of California, Davis, California 95616, USA
‡§ Lawrence Livermore Laboratory, University of California, Livermore, California 94550, USA

The distinctions between compact cores in various powerful extragalactic sources have proved difficult to interpret. In a few source categories (for example radio galaxies and quasistellar radio sources) extended structure on much larger scales exist; their energy is undoubtedly supplied through the narrow channels that are being increasingly observed and seem to be directed from the compact cores. Continuous production of high-energy plasma in a high-pressure region at the core centre is necessary to account for the energetics and channel structures[1]. The twin-exhaust mechanism[2] is one means of forming double jets in active galactic nuclei. As originally envisaged[2], the 'central engine' continuously releases hot gas in the centre of a flat-bottomed potential well formed by the stellar cluster in a galactic centre. This potential well holds a cloud of cooler gas which confines the hot gas in a central cavity. If the cooler gas cloud is flattened (for example, by rotation), buoyancy forces can accelerate the hot gas into two collimated jets via de Laval nozzles. These jets may correspond to the observed radio jets in quasars and radio galaxies, and result in the formation of extended double sources. Here, we combine new results from numerical calculations[5] of the Blandford–Rees model[2], with severe observational and theoretical constraints, to reach conclusions concerning the nature of the allowed flows. In particular, we conclude that high-velocity, high-powered jets cannot be produced in gravitational potentials produced by stellar clusters. However, the more general notion of the twin-exhaust mechanism[1], in which the central potential can be cusp-like near a massive black hole, is not ruled out for the high-powered radio sources. Note also that more compex twin-exhaust models (for example, magnetohydrodynamic flows) may lead to less severe constraints.

* Present address: Astronomy Program, University of Maryland, College Park, Maryland, USA.
‡ Present address: Max Planck Institut für Physik und Astrophysik, Institut für Astrophysik, Munich, FRG.

Blandford and Rees[2] obtained analytical results by treating the cavity flow as that of a one-dimensional relativistic fluid with the containing cloud supported by thermal pressure in a flat-bottomed potential well. They proposed central clouds of size $\lesssim 100$ pc. Wiita[3] demonstrated that a cloud as small as 1 pc is still consistent with X-ray observations. Furthermore, he also used a '$1\frac{1}{2}$' dimensional numerical method[4] to study the formation process and discovered a lower limit to the power for which jets form. Recently, a fully two-dimensional axisymmetric code has been used[5] to explore the formation process, with full inclusion of nonlinear hydrodynamic instabilities. Several interesting results were obtained and are summarized below.

A self-gravitating cloud with an axial pressure ratio of 2 : 1 was used and non-relativistic hot gas introduced with specific energy ~ 10 times greater than the cloud's specific energy, ε. For a certain central luminosity range ($L_{\min}$, $L_{\max}$), nozzles do form[5], but are more compact than those assumed previously[2–4]. Above $L_{\max} \sim 2.0\varepsilon^{5/2}G^{-1}$, the jet collapses and large clouds are ejected. Below $L_{\min} \sim 0.05\varepsilon^{5/2}G^{-1}$, the jet continuously pinches off and reforms and small bubbles rise out along the symmetry axis. These limits are also seen to be limits on the nozzle radius r_n—jets form when $0.1h < r_n < 0.6h$, where h is the pressure scale height in the cloud. These results were analytically generalized by careful consideration of the cavity structure and instabilities (for details see ref. 6). The lower limit is due to the Kelvin–Helmholtz instability breaking up thin nozzles, whereas the upper limit is due to the Rayleigh–Taylor instability along the cavity walls. Thus we found that jets form between

$$\frac{L_{\max}}{10^{46}\,\mathrm{erg\,s^{-1}}} = 2.0\xi\left(\frac{c_1}{3c_0}\right)\left(\frac{10^7 M_g}{M_t}\right)\left(\frac{c_0}{10^4\,\mathrm{km\,s^{-1}}}\right)^5 \quad (1)$$

and

$$\frac{L_{\min}}{10^{46}\,\mathrm{erg\,s^{-1}}} = 0.07\xi\left(\frac{c_1}{3c_0}\right)^{7/3}\left(\frac{10^7 M_g}{M_t}\right)\left(\frac{c_0}{10^4\,\mathrm{km\,s^{-1}}}\right)^5 \quad (2)$$

where c_0 and c_1 are the sound speeds in the cloud and hot gas, respectively; M_g and M_t are the mass of gas and total mass, respectively, within h; and $\xi c_0^2 = GM/h$, that is,

$$\frac{h}{1\,\mathrm{pc}} = 0.7\xi^{-1}\left(\frac{M_t}{10^{10}M_\odot}\right)\left(\frac{c_0}{10^4\,\mathrm{km\,s^{-1}}}\right)^{-2}. \quad (3)$$

These can be derived from $L \propto \rho_1 c_1^3 r_n^2$, where ρ_1 is the jet density[6]. The maximum follows directly from the condition $r_n < 0.6h$. The effectiveness of the Kelvin–Helmholtz instability results in the higher exponent of $(c_1/3c_0)$ in the minimum jet power (this extra exponent of 4/3 is a combination of jet thrust (2) and growth rate and phase velocity $(-2/3)$). It follows that jets cannot be maintained for $c_1 > 30c_0$.

We note the critical dependence on c_0. If c_0 typically varies between $10^3\,\mathrm{km\,s^{-1}}$ and $3.10^4\,\mathrm{km\,s^{-1}}$, then the jet power can

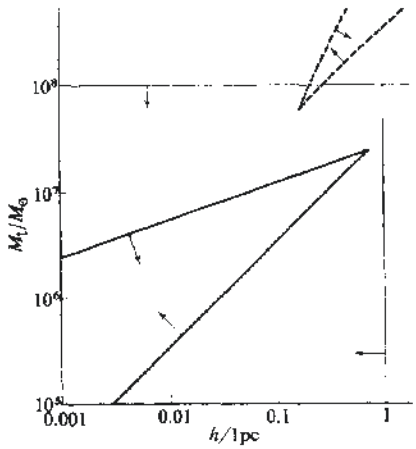


Fig. 1 The constraints on galactic nuclei mass M_t and scale height h for jets of power $10^{46}\,\mathrm{erg\,s^{-1}}$ in the optically thick case as described in the text. Both observational (solid lines) and theoretical constraints (broken lines) cannot be simultaneously satisfied.

©1981 Nature Publishing Group

range between 10^{41} erg s^{-1} and 10^{48} erg s^{-1}. Such a wide range is necessary to cover all sources with jets or extended components. We suggest that these formulae will also hold for a radiatively supported cloud, taking $c_0^2 \sim p_r/\rho$ where p_r is radiation pressure and ρ is the mass density, and also for a relativistic gas after adjustments are made for relativistic effects that will involve factors of $1-c_1^2/c^2$. Without the support of numerical simulations and given the complexity of three-dimensional fluid flows, these extensions are tentative.

We list below the observational constraints imposed by quasars and the compact central components of radio galaxies.

(1) $h < 1$ pc. This comes directly from very long baseline interferometry observations (there is also a class of radio galaxies with sizes of a few kpc that will not be considered here)[7].

(2) Collimated energy outputs, L_j, between 10^{41} erg s^{-1} and 10^{46} erg s^{-1} are typical over long time scales. The quasar jet in 4C 32.69 may require up to 10^{48} erg s^{-1} (ref. 8). Directed outbursts in strongly varying radio quasars often require 10^{48} erg s^{-1} over periods of a few years[9]. The upper end of the jet power range provides the severest constraint when combined with equation (1).

(3) X-ray luminosities from quasars are in the range $L_x \sim 10^{43}$–10^{47} erg s^{-1} (refs 10, 11). Only a fraction of this is thought to occur by thermal emission. Thus, although less extreme cases exist, we can place a severe limitation on quasars with jets by taking $L_{ff} \leq 0.1\ L_j$, where L_{ff} is the free–free emission from the cloud. This constraint will then also apply to radio galaxies.

To these we add the following theoretical constraints.

(4) $\rho_s = 10^9 M_\odot (1\text{ pc}/h)^{2/3}$ pc^{-3} is a maximum stellar density for ordinary stars[12,13], derived by requiring a star collision time $>10^8$ yr. Above this value, star mergers occur and the star cluster is rapidly converted into a supermassive star. This value is extremely high and we believe that the maximum ρ_s may in fact be smaller. Greater densities are possible if collapsed stars are present.

(5) Mass outflows from galactic nuclei $>\dot{M} \sim 1{,}000\ M_\odot$ yr^{-1} lead to enormous difficulties[1]. There is no known mechanism for continuously supplying the central engine at such a rate over long time scales. As $L_j = 24 c_0^2 \dot{M}$ (with $c_1 = 3c_0$), limits on $\dot{M}$ force limits on L_j.

Constraints (1) and (2) can be satisfied for a portion of the parameter space (M_g, M_t), given c_0, c_1 and ξ. It is convenient to rewrite constraint (1), using equation (3) as ($\xi = 1$, $c_1 = 3c_0$):

$$\frac{M_t}{10^{10} M_\odot} < 1.4 \left(\frac{c_0}{10^4 \text{ km s}^{-1}} \right)^2, \tag{4}$$

and to bound M_g by constraint (2) using equations (1) and (2):

$$\frac{M_g}{10^4 M_\odot} \simeq (0.05, 1.43) \left(\frac{M_t}{10^{10} M_\odot} \right) \left(\frac{c_0}{10^4 \text{ km s}^{-1}} \right)^{-5} \left(\frac{L_j}{10^{46} \text{ erg s}^{-1}} \right) \tag{5}$$

Near the limiting values, much of the flow is disrupted by instabilities, perhaps giving rise to the observed radio jets. Efficient energy transfer will occur in the range $\sim$(0.1, 0.7) of the bracketed quantity in equation (5), and we shall take the mean to be 0.4. We have also taken $c_1 = 3c_0$. Because $L_{min} \to L_{max}$ as $c_1 \to 30c_0$ this will not greatly affect our results.

First consider the case where the confining cloud is optically thin, that is, the optical depth, τ, of the cloud is less than unity. The thermal X-ray emission is given by[3]

$$\frac{L_{ff}}{L_j} \sim 3.10^{-2} \left(\frac{M_g}{10^4 M_\odot} \right) \left(\frac{10^{10} M_\odot}{M_t} \right)^2 \left(\frac{c_0}{10^4 \text{ km s}^{-1}} \right)^2 \times \left\{ 1 + 2.7 \left(\frac{c_0}{10^4 \text{ km s}^{-1}} \right)^2 \right\} \leq 0.1. \tag{6}$$

This constraint is stronger than the optical depth condition. When equations (4), (5) and (6) are combined, a lower limit to c_0 is obtained:

$$\frac{c_0}{10^4 \text{ km s}^{-1}} > 0.6 \left\{ 1 + 2.7 \left(\frac{c_0}{10^4 \text{ km s}^{-1}} \right)^2 \right\}^{1/5} \left(\frac{L_j}{10^{46} \text{ erg s}^{-1}} \right)^{1/5} \tag{7}$$

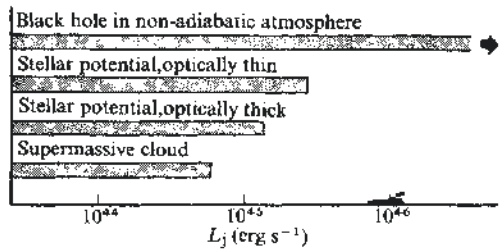


Fig. 2 The allowed luminosity range for various possible confining clouds.

An upper limit for $c_\odot$ is obtained by invoking constraint (4) and eliminating h using equation (3): $(c_0/10^4 \text{ km s}^{-1}) < 0.7 (M_t/10^{10} M_\odot)^{2/7}$. This yields the result that if we wish the flat-bottomed potential to be produced by stars, then $c_0 < 5.3 \times 10^3$ km s^{-1}. That is, the twin-exhaust model for a stellar cluster necessitates low sound speeds. Due to the restriction $c_1 < 30c_0$, stellar cluster models cannot produce the stable relativistic jets previously assumed[2,3]. Using equation (7), the maximum jet power is 2.7×10^{45} erg s^{-1}. These limits to c_0 and L_j may be related to head–tail radio galaxies and other weak radio sources, where low jet speeds have been inferred[14,15].

We can find further solutions involving stellar potentials if the cloud is optically thick. Here $c_0^2 \sim p_r/\rho \sim GM_t/h$ where p_r is the radiation pressure and ρ is the mass density. The median jet luminosity can be rewritten as ($c_1 = 3c_0$, $\xi = 1$):

$$\frac{L_j}{10^{46} \text{ erg s}^{-1}} \sim 1.6 \left(\frac{M_g}{10^7 M_\odot} \right) \left(\frac{M_t}{10^8 M_\odot} \right)^{3/2} \left(\frac{1 \text{ pc}}{h} \right)^{5/2}. \tag{8}$$

The total radiation limits M_t through the Eddington limit. Here we take

$$\frac{M_t}{10^8 M_\odot} = \frac{L_{edd}}{10^{46} \text{ erg s}^{-1}} < \frac{L_j}{10^{46} \text{ erg s}^{-1}}. \tag{9}$$

This proves to be unimportant in the following. Further constraints are $M_g \leq M_t$, and $M_g/10^7 M_\odot > 4.3 (h/1 \text{ pc})^2$ is the condition for the optical thickness of the jet to exceed 10 (if the cloud is optically thick, but the jet is optically thin, the advantages of taking an optically thick cloud are lost). For $M_g < M_t$, the optically thick and observational constraints (1–3) can be satisfied (Fig. 1) only if $M_t < 3 \times 10^7 M_\odot$ for the twin-exhaust model. The theoretical constraints (4, 5), however, require $M_t > 8.4 \times 10^7 M_\odot$ for $L_j = 10^{46}$ erg s^{-1}. Thus we find two possibilities: either $L_j < 1.4 \times 10^{45}$ erg s^{-1} or the mass is not in the form of ordinary stars. The second possibility necessitates masses of an order of magnitude above that given by constraint (4). Thus, again we have found that stellar cluster models are implausible for high powered jets.

Finally, we can look at supermassive clouds by taking $M_g = M_t$ and so dropping constraint (4). Use of constraint (5) in equation (8) yields $L_j < 6 \times 10^{44}$ erg s^{-1}, after eliminating h using equation (3). Here, the low sound speed of the dense cloud is prohibiting powerful jets.

There are two alternatives to assuming that M_t is in the form of stars. The first is to have the mass in a cluster of collapsed objects. With the increased collision times, constraint (4) can be relaxed, but we will not pursue this possibility here. The other is that the mass is primarily in a central black hole that will produce a cusp-like potential ($1/r$). Such supermassive objects can meet the mass requirements of either of the above models and are consistent with observations[16].

Can jets form in steep potential wells? The pressure distribution of a stationary adiabatic atmosphere surrounding a point mass is of the form $P \propto r^{-(\gamma/\gamma-1)} \propto r^{-5/2}$ for a specific heat ratio $\gamma = 5/3$ where r is the radial distance. It was found[6] that the cavity structures analysed here will only be produced for $P \propto r^{-m}$ with $m < 2$. Thus adiabatic atmospheres are not permissible. A radiatively cooling cloud will have a flatter pressure distribution. With pressure dominating gravity, the mass requirements are eased; moreover, the rate of cooling leads to a central accretion

©1981 Nature Publishing Group

rate consistent with the mass ejected through the jets[6]. We further suggest that the cloud sound speed is $\sim 10^4$ km s^{-1}, as then the jet velocity will be nonrelativistic, $\sim 0.1c$, which agrees with expectations[1,17]. This model predicts that jets approaching relativistic speeds, that is, $c_1 \rightarrow 30c_0 \sim L_{\min} \rightarrow L_{\max}$, will be highly variable and short-lived, perhaps giving rise to the rapidly separating discreet components observed in such sources, and intrinsic outbursts with $\geq 10^{47}$ erg s^{-1}.

We conclude that the twin-exhaust model for radio jets cannot be ruled out, but that distinct classes of confining clouds (Fig. 2) may occur. The low-powered jets ($L_j \leq 10^{45}$ erg s^{-1}) can be maintained by a flat-bottomed stellar cluster potential. These jets must have nonrelativistic jet velocities, which could be as low as 10^2–10^3 km s^{-1}, comparable with the interstellar velocities which the jets may encounter on the way out of the 'central engine'. Thus, these low-power jets could still have black hole sources ($r \sim 10^{-5}$ pc), but with the jet flow becoming randomized before being refocused by de Laval nozzles on scales of ~ 1 pc where the gravitational potential is dominated by the stellar cluster. It seems that if the stars are replaced by a central black hole with a cusp potential and a non-adiabatic atmosphere, then powerful jets are attainable. It is hoped that the above analysis will suggest future observations which will distinguish between these models.

L.S. thanks Martin Rees for his hospitality and stimulating discussions at the Institute of Astronomy, Cambridge, where part of this work was done. We thank F. K. Lamb for valuable ideas and criticisms on major portions of the paper. We also appreciate valuable discussions with R. D. Blandford, D. Lynden Bell, G. Miley and P. Wilta, and thank the Department of Energy and the NSF for financial support under grants PHY 78-04404 and PHY 80-01496. L.S. is an Alfred P. Sloan Fellow.

Received 20 May; accepted 4 August 1981.

1. Rees, M. J. *IAU Symp.* **94** (1980).
2. Blandford, R. D. & Rees, M. J. *Mon. Not. R. astr. Soc.* **169**, 395 (1974).
3. Wilta, P. J. *Astrophys. J.* **221**, 41 (1978).
4. Wilta, P. J. *Astrophys. J.* **221**, 436 (1978).
5. Norman, M. L., Smarr, L., Wilson, J. R. & Smith, M. D. *Astrophys. J.* (in the press).
6. Smith, M. D., Smarr, L., Norman, M. L. & Wilson, J. R. *Astrophys. J.* (in the press).
7. Miley, G. K. *A. Rev. Astr. Astrophys.* **18**, 165 (1980).
8. Potash, R. I. & Wardle, J. F. C. *Astrophys. J.* **239**, 42 (1980).
9. Burbidge, G. *Proc. IAU Symp.* **44** (1974).
10. Tananbaum, H. *et al. Astrophys. J.* **234**, 9 (1979).
11. Ku, W.H.-M., Helfand, D. J. & Lucy, L. B. *Nature* **288**, 323 (1980).
12. Begelman, M. C. & Rees, M. J. *Mon. Not. R. astr. Soc.* **185**, 847 (1978).
13. Spitzer, L. & Saslaw, W. C. *Astrophys. J.* **143**, 400 (1966).
14. Blandford, R. D. & Icke, V. *Mon. Not. R. astr. Soc.* **185**, 527 (1978).
15. Perley, R. A., Willis, A. G. & Scott, J. S. *Nature* **281**, 437 (1979).
16. Young, P. J., Sargent, W. L. W., Kristian, J. & Westphal, J. A. *Astrophys. J.* **234**, 76 (1979).
17. van Groningen, E., Miley, G. K. & Norman, C. A. *Astr. Astrophys.* **90**, L7 (1980).

Glass formation in ionic systems

Marcel Poulain

Laboratoire de Chimie Minérale D, Laboratoire Associé au CNRS No. 254, Université de Rennes, Campus de Beaulieu, Avenue du Général Leclerc, 35042 Rennes Cedex, France

In the past five years, glass formation has been observed in many chemical systems involving zirconium tetrafluoride[1–5]. These ionic glasses were unexpected as no theory of glass formation had predicted their occurrence. Most common glasses can be explained by the Zachariazen theory[6] which gives criteria for vitreous structures with highly directed three-dimensional bond arrays, according to energy and kinetic considerations. However, the theory does not encompass some new amorphous systems such as amorphous germanium or the new ionic glasses. I review here the structural and energetic conditions for glass formation in ionic systems with particular reference to fluoride glasses.

In some non-stoichiometric compounds, especially in 'anion-excess' phases, the structure includes both order and disorder elements, the cations describing a regular network related to the average crystallographic cell and the anions being situated in a disordered way over equivalent positions around the cationic sites. Examples are UO_{2+x} (ref. 7), $(CaY)F_{2+x}$ (ref. 8), MF_{2+x} (ref. 9) and (Zr, Ln) (O, F)$_{3+x}$ (ref. 10). Which all have cubic symmetry. A cubic distribution maximizes the cation–cation distances and therefore minimizes their coulombic repulsion. If this regular cubic distribution may be precluded, for example, by addition of larger cations, then the cationic array may also be disordered. Such a relationship exists between the non-stoichiometric phrases (Ln, Zr)F_{3+x} (ref. 11) and the ternary ZrF_4–LnF_3–BaF_2 glasses (ref. 12).

The predominant role of the anions in disordered ionic solid state phases enables the problem of glass formation to be addressed by considering the additional features leading to stabilization of a non-periodic packing. This approach involves both energetic and ordering elements. Glass formation is allowed if the rate of nucleus formation and the velocity of crystal growth are low enough to avoid noticeable recrystallization of the melt between liquidus and glassy transition. This may be achieved when the activation enthalpy for shear viscosity is high. In the case of covalent network glasses, the structural implications are expressed by Zachariasen rules. For ionic glasses, the first obvious condition is that the mobility of highly charged cations in the structure is low. Besides, constructing a non-periodic structure implies that there are several ways in which the cations can be inserted in the anionic packing, which is also correlated to the fact that the energy of the glassy structure must be close to the energy of the crystalline forms that derive from it.

The lattice energy of the solid W_S may be written as: $W_S = W_E + W_R$ where W_E is the electrostatic energy and W_R the repulsion energy resulting from the overlapping of the electronic shells. The electrostatic term W_E may be rigorously calculated by summation of convergent series in direct or reciprocal space if the precise structure is known[13]. It may be expressed as the sum of the repulsive anionic energy W_{RA}, the repulsive cationic energy W_{RC}, and the interaction energy between ions of opposite sign W_I.

$$W_E = W_I + W_{RA} + W_{RC}$$

with $W_I < 0$, W_{RA} and $W_{RC} > 0$.

The predominant part is W_I which is proportional to the product of the cationic charge n and the anionic charge z. W_{RA} is proportional to z^2 and W_{RC} to n^2. W_E will increase with increasing n, and decreasing bond lengths, as long as the repulsive part W_{RC} is not too important. In a vitreous ionic structure, only a short-range order exists and therefore the coulombic energy restricted to near-neighbour ions is likely to be similar for crystals and glasses. The medium- and long-range coulombic

Table 1 Glass forming ability of various cations with respect to anionic and cationic field strength

Cation	Anion	F_A*	F_C*	F_A/F_C	Glass progenitor	Ref.
Al^{3+}	F	0.78	5.6	7.2	Yes	19
Be^{2+}	F	0.78	7.4	9.5	Yes	19
Zr^{4+}	F	0.78	5	6.4	Yes	12
Hf^{4+}	F	0.78	5.2	6.7	Yes	20
Ga^{3+}	F	0.78	4.8	6.1	Yes	14
Fe^{3+}	F	0.78	4.7	6.0	Yes	14
Cr^{3+}	F	0.78	4.9	6.3	Yes	14
Th^{4+}	F	0.78	3.8	4.9	Yes	15, 16
Y^{3+}	F	0.78	3.1	4.0	Yes	21, 22
Zn^{2+}	F	0.78	2.8	3.6	Yes	22
Si^{4+}	F	0.78	15.4	19.7	No	
Mo^{6+}	F	0.78	14.6	18.7	No	
Ca^{2+}	F	0.78	1.78	2.3	No	
NaF	F	0.78	0.85	1.1	No	
Zn^{2+}	Cl	0.55	3.33	6.0	Yes	19
Bi^{3+}	Cl	0.55	2.91	5.3	Yes	23

* Calculated from the ionic radius values given in ref. 24.

©1981 Nature Publishing Group